



Solar-driven, highly sustained splitting of seawater into hydrogen and oxygen fuels

Yun Kuang^{a,b,c,1}, Michael J. Kenney^{a,1}, Yongtao Meng^{a,d,1}, Wei-Hsuan Hung^{a,e}, Yijin Liu^f, Jianan Erick Huang^a, Rohit Prasanna^g, Pengsong Li^{b,c}, Yaping Li^{b,c}, Lei Wang^{h,i}, Meng-Chang Lin^d, Michael D. McGehee^{g,j}, Xiaoming Sun^{b,c,d,2}, and Hongjie Dai^{a,2}

^aDepartment of Chemistry, Stanford University, Stanford, CA 94305; ^bState Key Laboratory of Chemical Resource Engineering, Beijing University of Chemical Technology, Beijing 100029, China; ^cBeijing Advanced Innovation Center for Soft Matter Science and Engineering, Beijing University of Chemical Technology, Beijing 100029, China; ^dCollege of Electrical Engineering and Automation, Shandong University of Science and Technology, Qingdao 266590, China; ^eDepartment of Materials Science and Engineering, Feng Chia University, Taichung 40724, Taiwan; ^fStanford Synchrotron Radiation Light Source, SLAC National Accelerator Laboratory, Menlo Park, CA 94025; ^gDepartment of Materials Science and Engineering, Stanford University, Stanford, CA 94305; ^hCenter for Electron Microscopy, Institute for New Energy Materials, Tianjin University of Technology, Tianjin 300384, China; ⁱTianjin Key Laboratory of Advanced Functional Porous Materials, School of Materials, Tianjin University of Technology, Tianjin 300384, China; and ^jDepartment of Chemical Engineering, University of Colorado Boulder, Boulder, CO 80309

Contributed by Hongjie Dai, February 5, 2019 (sent for review January 14, 2019; reviewed by Xinliang Feng and Ali Javey)

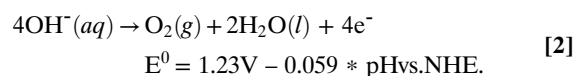
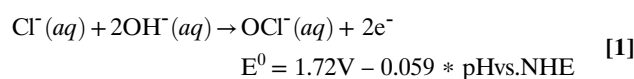
Electrolysis of water to generate hydrogen fuel is an attractive renewable energy storage technology. However, grid-scale freshwater electrolysis would put a heavy strain on vital water resources. Developing cheap electrocatalysts and electrodes that can sustain seawater splitting without chloride corrosion could address the water scarcity issue. Here we present a multilayer anode consisting of a nickel-iron hydroxide (NiFe) electrocatalyst layer uniformly coated on a nickel sulfide (NiSx) layer formed on porous Ni foam (NiFe/NiSx-Ni), affording superior catalytic activity and corrosion resistance in solar-driven alkaline seawater electrolysis operating at industrially required current densities (0.4 to 1 A/cm²) over 1,000 h. A continuous, highly oxygen evolution reaction-active NiFe electrocatalyst layer drawing anodic currents toward water oxidation and an in situ-generated polyatomic sulfate and carbonate-rich passivating layers formed in the anode are responsible for chloride repelling and superior corrosion resistance of the salty-water-splitting anode.

seawater splitting | hydrogen production | electrocatalysis | anticorrosion | solar driven

Storing renewable energy by driving uphill chemical reactions is an attractive solution to the intermittency problem faced by many alternative energy sources (1, 2). Due to its high gravimetric energy density (142 MJ/kg) and pollution-free use, hydrogen is considered one of the most promising clean energy carriers (3–5). Electrolysis of water is a clean way to generate hydrogen at the cathode but is highly dependent on efficient and stable oxygen evolution reaction (OER) at the anode (6–10). However, if water splitting is used to store a substantial portion of the world's energy, water distribution issues may arise if vast amounts of purified water are used for fuel formation. Seawater is the most abundant aqueous electrolyte feedstock on Earth but its implementation in the water-splitting process presents many challenges, especially for the anodic reaction.

The most serious challenges in seawater splitting are posed by the chloride anions (~0.5 M in seawater). At acidic conditions, the OER equilibrium potential vs. the normal hydrogen electrode (NHE) is only higher than that of chlorine evolution by 130 mV (11), but OER is a four-electron oxidation requiring a high overpotential while chlorine evolution is a facile two-electron oxidation with a kinetic advantage. While chlorine is a high-value product, the amount of chlorine that would be generated to supply the world with hydrogen would quickly exceed demand (12). Unlike OER, the equilibrium potential of chlorine evolution does not depend on pH. Selective OER over chlorine generation can thus be achieved in alkaline electrolytes to lower the onset of OER. However, hypochlorite formation could still compete with OER (Eqs. 1 and 2; both are pH-dependent) (11), with an onset

potential ~490 mV higher than that of OER, which demands highly active OER electrocatalysts capable of high-current (~1 A/cm²) operations for high-rate H₂/O₂ production at overpotentials well below hypochlorite formation:



Even with a highly active OER catalyst in alkaline electrolytes, the aggressive chloride anions in seawater can corrode many catalysts and substrates through metal chloride-hydroxide formation mechanisms (13):

Significance

Electrolysis of water to generate hydrogen fuel could be vital to the future renewable energy landscape. Electrodes that can sustain seawater splitting without chloride corrosion could address the issue of freshwater scarcity on Earth. Herein, a hierarchical anode consisting of a nickel-iron hydroxide electrocatalyst layer uniformly coated on a sulfide layer formed on Ni substrate was developed, affording superior catalytic activity and corrosion resistance in seawater electrolysis. In situ-generated polyanion-rich passivating layers formed in the anode are responsible for chloride repelling and high corrosion resistance, leading to new directions for designing and fabricating highly sustained seawater-splitting electrodes and providing an opportunity to use the vast seawater on Earth as an energy carrier.

Author contributions: Y.K., M.J.K., and H.D. designed research; Y.K., M.J.K., Y.M., W.-H.H., Y. Liu, J.E.H., R.P., P.L., Y. Li, L.W., and M.-C.L. performed research; Y.K., M.J.K., Y.M., W.-H.H., Y. Liu, J.E.H., R.P., P.L., Y. Li, L.W., M.-C.L., M.D.M., X.S., and H.D. analyzed data; and Y.K., M.J.K., and H.D. wrote the paper.

Reviewers: X.F., Technische Universität Dresden; and A.J., University of California, Berkeley.

Conflict of interest statement: A provisional patent (US 62/630,599) has been filed related to this work.

This open access article is distributed under [Creative Commons Attribution-NonCommercial-NoDerivatives License 4.0 \(CC BY-NC-ND\)](https://creativecommons.org/licenses/by-nc-nd/4.0/).

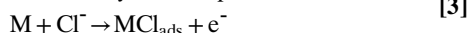
¹Y.K., M.J.K., and Y.M. contributed equally to this work.

²To whom correspondence may be addressed. Email: sunxm@mail.buct.edu.cn or hdai1@stanford.edu.

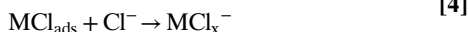
This article contains supporting information online at www.pnas.org/lookup/suppl/doi:10.1073/pnas.1900556116/-DCSupplemental.

Published online March 18, 2019.

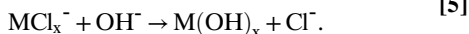
Adsorption of Cl^- by surface polarization :



Dissolution by further coordination :



Conversion from chloride to hydroxide



To avoid relying on costly desalination processes, development of electrodes that are corrosion-resistant for splitting seawater into H_2 and O_2 is crucial to the advancement of seawater electrolysis, an undertaking with limited success thus far. Mn-based oxides deposited on IrO_2 -Ti showed stability for OER in NaCl-containing electrolytes but were limited by Ir's high cost (14–16). NiFe-layered double hydroxide (NiFe-LDH) (17), Co-borate, and Co-phosphate materials have all shown high OER activity in NaCl-containing electrolytes, but long-term stability at industrial current densities $\sim 1 \text{ A/cm}^2$ has not been achieved for seawater electrolysis (11, 18, 19).

This work developed a multilayer electrode that upon activation evolved into a polyanion sulfate/carbonate-passivated NiFe/NiS_x-Ni foam anode with high activity and corrosion resistance for OER in chloride-containing alkaline electrolytes. The negatively charged polyanions incorporated into the anode were derived from anodization of the underlying nickel sulfide layer and carbonate ions in the alkaline solution, repelling Cl^- anions in seawater and hence imparting corrosion resistance. When the anode is paired with an advanced Ni-NiO-Cr₂O₃ hydrogen evolution cathode in alkaline seawater, the electrolyzer can operate at low voltages and high currents and last for more than 1,000 h.

The NiFe/NiS_x-Ni foam anode (referred to as Ni³ for brevity) was made by first converting the surface of Ni foam to NiS_x by devising a solvothermal reaction of Ni foam with elemental sulfur in toluene (*SI Appendix, Materials and Methods*). After formation of the NiS_x layer, an OER-active NiFe hydroxide (20–24) was electrodeposited via the reduction of nitrate from a solution of $\text{Ni}(\text{NO}_3)_2$ and $\text{Fe}(\text{NO}_3)_3$ (Ni:Fe = 3:1) (Fig. 1A) (20, 25). We propose that the matched crystalline phase and *d* spacing could allow epitaxial growth of NiFe hydroxide laminates on NiS_x surface, resulting in a uniform coating of vertically grown LDH on top of the NiS_x layer (Fig. 1C and *SI Appendix, Fig. S1*). Electron diffraction patterns revealed that the NiS_x and NiFe layers were amorphous in nature (*SI Appendix, Fig. S1*). SEM (Fig. 1B and C) and cross-sectional elemental mapping revealed a ~ 1 - to 2 - μm -thick NiS_x layer formed on Ni foam (*SI Appendix, Fig. S2*), with a ~ 200 -nm-thick NiFe layer on top of the NiS_x layer (Fig. 1D and E).

After anodic activation of the Ni³ anode in an alkaline simulated seawater electrolyte (1 M KOH plus 0.5 M NaCl, a mimic of seawater adjusted to alkaline), OER performance was measured in a three-electrode configuration in a freshly prepared alkaline simulated seawater electrolyte (Fig. 2A). Cyclic voltammetry (CV) showed a 30 mV lower onset overpotential (taken to be the potential vs. RHE where the reverse scan reaches 0 mA/cm^2), an improvement over the original electrodeposited NiFe catalyst and NiFe-LDH (17, 20, 21). The large increase in the $\text{Ni}^{2+} \rightarrow \text{Ni}^{3+}$ oxidation peak ($\sim 1.44 \text{ V}$; Fig. 2A) suggested increased electrochemically active nickel sites for OER through the activation process. A high current density of 400 mA/cm^2 at an overpotential of $\eta = 510 \text{ mV}$ was reached (no iR compensation, $R = 0.7 \pm 0.05 \text{ ohm}$; Fig. 2B). After iR compensation, the actual overpotential applied on the Ni³ anode to achieve an OER current density of 400 mA/cm^2 was $\sim 0.3 \text{ V}$, well below the 0.49 V overpotential required to trigger chloride oxidation to hypochlorite.

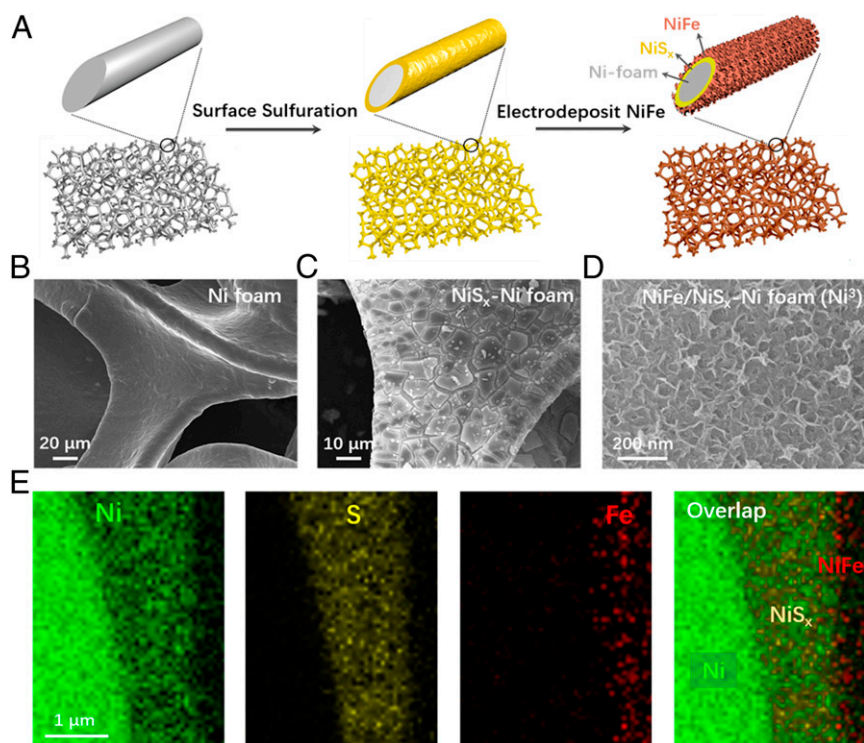


Fig. 1. Fabrication and structure of the dual-layer NiFe/NiS_x-Ni foam (Ni³) anode for seawater splitting. (A) Schematic drawing of the fabrication process, including a surface sulfuration step and an in situ electrodeposition of NiFe. (B–D) SEM images of untreated nickel foam, NiS_x formed on nickel foam, and electrodeposited NiFe on the NiS_x surface. (E) Elemental mapping of a cross-section of NiFe/NiS_x on a Ni wire in the Ni foam, revealing Ni wire, NiS_x, and NiFe layers.

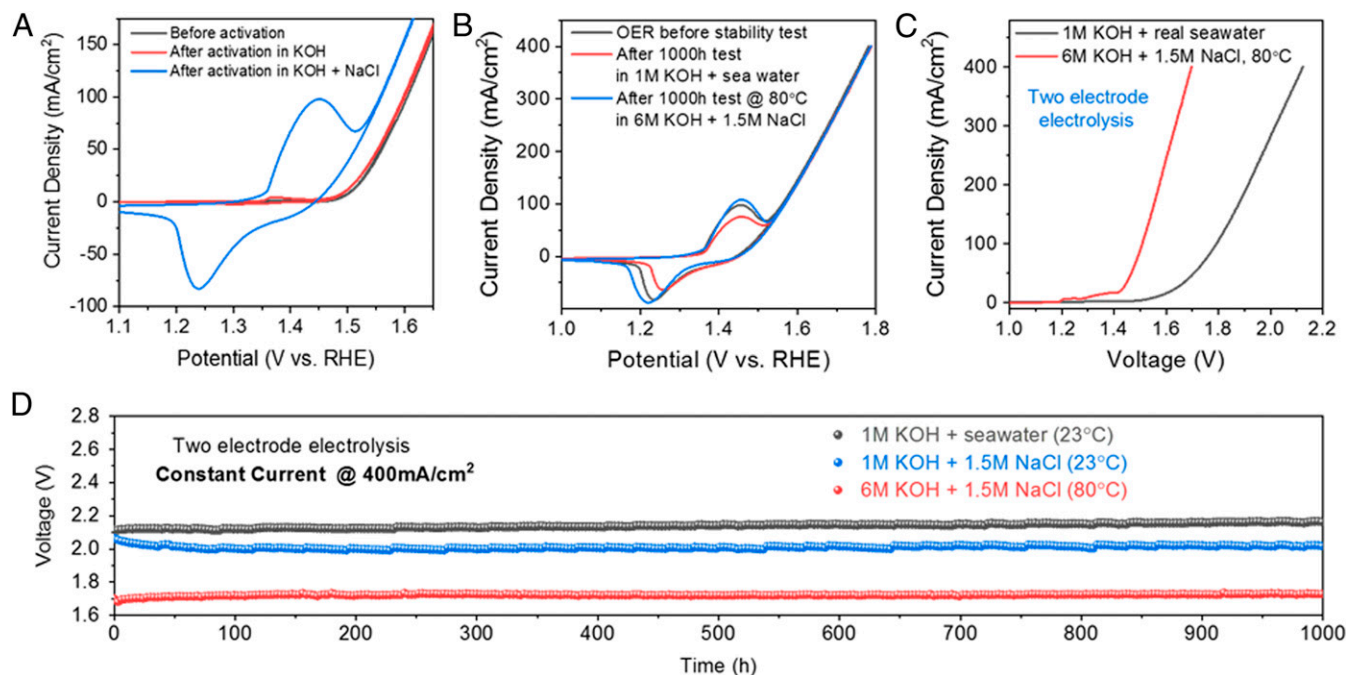


Fig. 2. Sustained, energy-efficient seawater splitting continuously over 1,000 h. (A) CV scans of a Ni^3 anode before and after activation in 1 M KOH at 400 mA/cm^2 for 12 h and 1 M KOH + 0.5 M NaCl for 12 h at 400 mA/cm^2 ; the CV curves were taken in 1 M KOH, resistance $0.75 \pm 0.05 \text{ ohm}$. (B) CV scans of a Ni^3 anode (activated in 1 M KOH at 400 mA/cm^2 for 12 h followed by 1 M KOH + 0.5 M NaCl at 100 mA/cm^2 for 12 h) before and after 1,000-h seawater splitting in an alkaline simulated seawater electrolyte (1 M KOH with 0.5 M NaCl in deionized water), $R = 0.7 \pm 0.05 \text{ ohm}$. (C) Linear sweep voltammetry (LSV) scans of a seawater-splitting electrolyzer (Ni^3 paired with a $\text{Ni-NiO-Cr}_2\text{O}_3$ cathode) taken in alkaline seawater electrolyte (1 M KOH + real seawater) at room temperature (23°C , resistance $0.95 \pm 0.05 \text{ ohm}$) and in near-saturated salt concentration (1.5 M NaCl) under industrial electrolysis conditions (6 M KOH electrolyte at 80°C , resistance $0.55 \pm 0.05 \text{ ohm}$). The Ni^3 anode was first activated under 400 mA/cm^2 in 1 M KOH for 12 h followed by 1 M KOH + 0.5 M NaCl at 100 mA/cm^2 for 12 h. (D) Durability tests (1,000 h) recorded at a constant current of 400 mA/cm^2 of the seawater-splitting electrolyzer under 1 M KOH + real seawater at room temperature ($R = 0.95 \pm 0.05 \text{ ohms}$), 1 M KOH + 1.5 M NaCl at room temperature ($R = 0.8 \pm 0.05 \text{ ohms}$), and 6 M KOH electrolyte at 80°C ($R = 0.55 \pm 0.05 \text{ ohms}$), respectively. Data were recorded after activation of Ni^3 anode under 400 mA/cm^2 in both 1 M KOH and 1 M KOH + 0.5 M NaCl (or 1.5 M NaCl for the test in 1 M/6 M KOH + 1.5 M NaCl) electrolytes for 12 h.

We then paired the activated/passivated Ni^3 anode with a highly active $\text{Ni-NiO-Cr}_2\text{O}_3$ hydrogen evolution reaction (HER) cathode (26) for two-electrode high-current electrolysis of alkaline seawater. Three-electrode linear scan voltammetry of the $\text{Ni-NiO-Cr}_2\text{O}_3$ showed that $\sim 0.37 \text{ V}$ overpotential was required to drive an HER current density of 500 mA/cm^2 (SI Appendix, Fig. S3A, without iR compensation). After iR compensation, the overpotential applied on the catalyst to drive a current density of 500 mA/cm^2 was as low as $\sim 160 \text{ mV}$, which was among the best nonprecious-metal-based HER catalysts reported so far. In addition, chloride did not degrade the activity and stability during the HER process (SI Appendix, Fig. S3B). The two-electrode electrolysis experiment was first carried out in 1 M KOH added to seawater from the San Francisco Bay at room temperature (23°C). The electrolyzer operated at a current density of 400 mA/cm^2 under a voltage of 2.12 V (Fig. 2C, without iR compensation; $R = 0.95 \pm 0.05 \text{ ohm}$) continuously for more than 1,000 h without obvious decay (Fig. 2D), corroborated by three-electrode measurements before and after the 1,000-h stability test (Fig. 2B).

In a real electrolysis application, salt may accumulate in the electrolyte if seawater is continuously fed to the system and water is converted to H_2 and O_2 . To this end, we investigated electrolytes with higher NaCl concentrations than in seawater, using deionized water with 1 M KOH + 1 M NaCl or even 1.5 M NaCl (Fig. 2D and SI Appendix, Fig. S4). Meanwhile we increased NaCl concentration during Ni^3 anodic activation/passivation to match the conditions of the stability test (i.e., the second phase of anodization would use 1 M KOH + 1 M or 1.5 M NaCl if the stability test was going to be carried out in this electrolyte). Due to the higher ionic strengths with NaCl concentrations of 1 M and

1.5 M, the cell resistance decreased and the voltages of the electrolyzers using the activated Ni^3 anode afforded a current density of 400 mA/cm^2 at lower cell voltages of 2.09 V and 2.02 V, respectively. The electrolysis was still stable for more than 1,000 h, with no obvious corrosion or voltage increase observed, suggesting impressively active and stable anode for electrolysis in high-salinity water. Further, the electrolyzer operated stably under conditions typically used in industry (high temperature and concentrated base) (27), needing only 1.72 V to reach a current density of 400 mA/cm^2 in 6 M KOH + 1.5 M NaCl at 80°C for $>1,000 \text{ h}$ (Fig. 2C and D). Mass spectrometry showed no anodic Cl_2 evolution and gas chromatography showed a relative Faradaic efficiency (R_{FE} , defined as the ratio of O_2 produced in KOH + NaCl electrolyte over O_2 produced in KOH electrolyte) of O_2 production of $\sim 100\%$ (SI Appendix, Figs. S5 and S6), suggesting selective OER in alkaline-adjusted salty water using the passivated Ni^3 anode.

We performed control experiments and found that in a “harsh” electrolyte of 1 M KOH with a high concentration of 2 M NaCl, an activated Ni^3 anode paired with a $\text{Ni-NiO-Cr}_2\text{O}_3$ cathode lasted for $\sim 600 \text{ h}$ (SI Appendix, Fig. S7A) before breakdown under a constant current of 400 mA/cm^2 (during which R_{FE} was $\sim 99.9\%$ for O_2 ; SI Appendix, Fig. S7C). Bare Ni foam and sulfur-treated Ni foam (to form NiS_x) without NiFe lasted for less than 20 min (SI Appendix, Fig. S7A, Inset) with $R_{\text{FE}} < 35\%$ for O_2 (SI Appendix, Fig. S7C). NiFe hydroxide-coated Ni foam without the NiS_x interlayer was also inferior to Ni^3 and lasted 12 h (SI Appendix, Fig. S7A) with an R_{FE} for O_2 of 99% at 400 mA/cm^2 (SI Appendix, Fig. S7C). These results together with three-electrode constant voltage testing (SI Appendix, Fig. S7D) suggested that the

combination of NiFe hydroxide on top of NiS_x/Ni to form a Ni³ structure was key to superior chloride corrosion resistance.

The electrode structures (before and after seawater splitting in various electrolytes) were investigated by 3D X-ray microtomography (SI Appendix, Fig. S8). After 1,000 h of seawater electrolysis, the Ni³ anode showed a structural integrity (SI Appendix, Fig. S8B) similar to that before electrolysis (SI Appendix, Fig. S8A). Even under a harsh condition with four times the salt concentration of real seawater for 300 h, the anode still maintained the Ni foam skeleton structure (SI Appendix, Fig. S8C). However, Ni foam without NiS_x but with electrodeposited NiFe (the best control sample) showed severe corrosion after only an 8-h test in 1 M KOH + 2 M

NaCl (SI Appendix, Fig. S8D). Clearly, both the NiFe OER catalyst coating and the nickel sulfide layer underneath the catalyst are critical to long-term stability of the anode against chloride corrosion.

Given that the activated Ni³ anodes were quite stable in various electrolytes under the current density of 400 mA/cm², we then tested the system at even higher current densities. Three-electrode testing of an activated Ni³ electrode in simulated alkaline seawater electrolyte showed a 750 mV overpotential (without iR compensation) for reaching a high OER current density of 1,500 mA·cm⁻² (Fig. 3A). After iR compensation, the actual overpotential applied on the Ni³ anode to achieve the OER current density of 1500 mA/cm² in simulated alkaline seawater was ~0.38 V (Fig. 3B), still

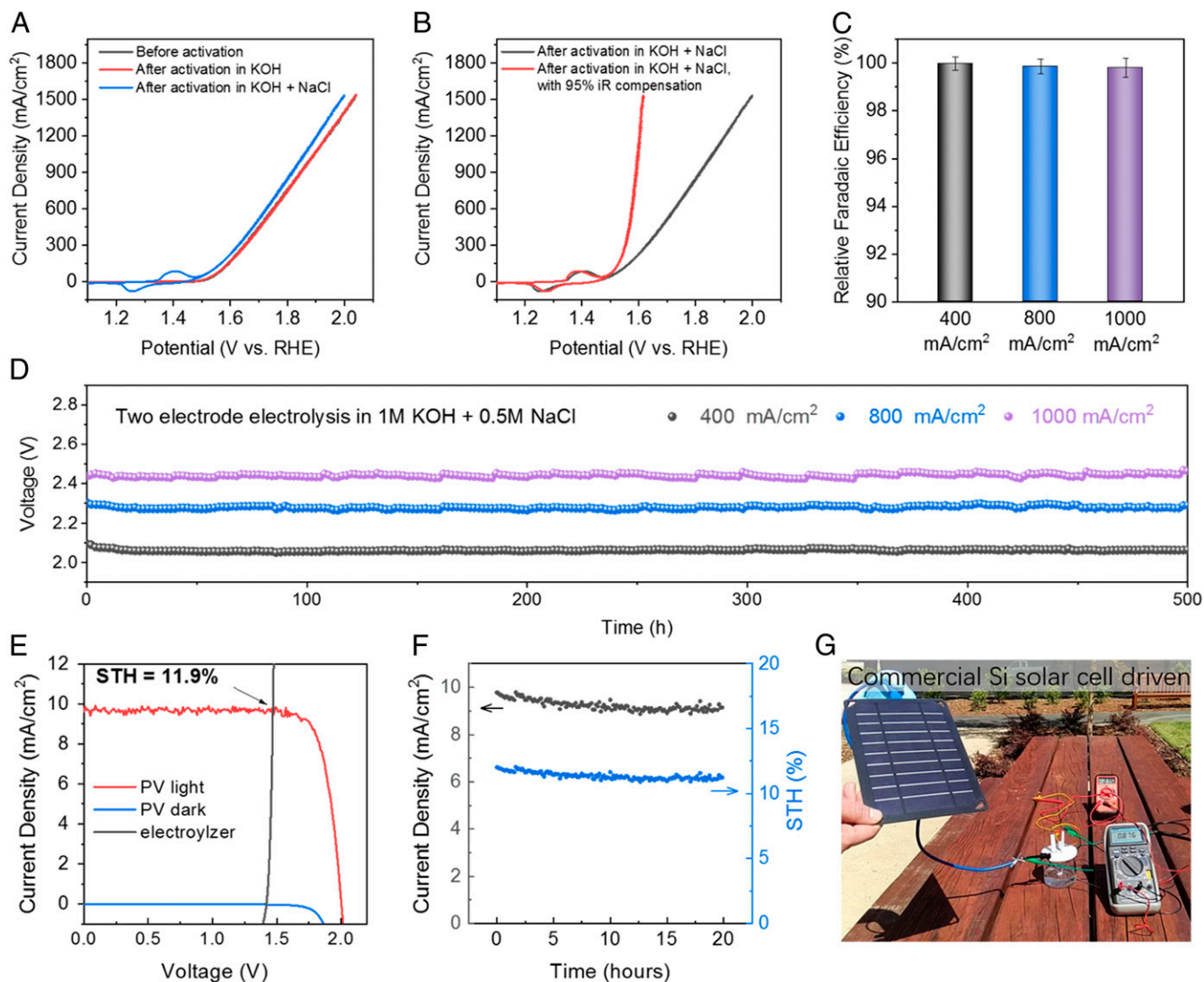


Fig. 3. Seawater electrolysis running at current density up to 1 A/cm². (A) CV scans of a 0.25-cm² Ni³ anode before and after activation in 1 M KOH and 1 M KOH + 0.5 M NaCl (both at 400 mA/cm²); the CV curves were taken in simulated alkaline seawater (1 M KOH + 0.5 M NaCl), resistance 1.2 ± 0.05 ohm. (B) CV scans with and without iR compensation of the 0.25-cm² Ni³ anode shown in A. (C) Two electrode R_FEs of oxygen generation in seawater electrolyzer (Ni³ paired with Ni-NiO-Cr₂O₃) running at 400 mA/cm², 800 mA/cm², and 1,000 mA/cm² in 1 M KOH + 0.5 M NaCl electrolyte. (D) Durability tests of the seawater-splitting electrolyzer (0.5 cm² Ni³ paired with Ni-NiO-Cr₂O₃) recorded in 1 M KOH + 0.5 M NaCl electrolyte at room temperature under constant currents of 400 mA/cm² ($R = 1.5 \pm 0.05$ ohms), 800 mA/cm² ($R = 1.6 \pm 0.05$ ohms), and 1,000 mA/cm² ($R = 1.6 \pm 0.05$ ohms), respectively. Data were recorded after activation of Ni³ anode under 400 mA/cm² in both 1 M KOH and 1 M KOH + 0.5 M NaCl electrolytes for 12 h. (E) Current density–potential curve (J–V) of the seawater electrolyzer and two perovskite tandem cells under dark and simulated AM 1.5-G 100 mW·cm⁻² illumination. The illuminated surface area of each perovskite cell was 0.12 cm² (0.24 cm² total), and the catalyst electrode areas (geometric) were 1 cm² each. The Ni³ were first activated in 1 M KOH under 400 mA/cm² for 12 h then in 1 M KOH + 0.5 M NaCl under 100 mA/cm² for 12 h. After that the electrolyzer was held at 20 mA/cm² for 5 h before pairing with the solar cell. (F) Twenty-hour stability test of perovskite solar cell-driven seawater electrolysis and corresponding solar-to-hydrogen (STH) efficiency. (G) A photo showing a commercial silicon solar cell-driven electrolysis (1-cm² electrodes) of seawater running at 876 mA under a voltage of 2.75 V ($R = 1.0 \pm 0.05$ ohms). No iR compensation was applied to any experiment.

with a low degree of crystallinity (*SI Appendix, Fig. S1F*; the electron diffraction pattern did reveal ~ 0.64 -nm layer spacing). Indeed, TOF secondary ion mass spectrometry (TOF-SIMS) mapping on a Ni³⁺ electrode after activation unambiguously revealed the presence of both sulfate and carbonate species (Fig. 4D), confirming the formation of a layer of NiFe-LDH intercalated with two types of polyanions (32, 33).

Further, we performed Raman spectroscopy to investigate the fate of the NiS_x interlayer underneath the NiFe-based catalyst by activating an NiS_x-coated Ni foam electrode under the same anodic activation process used for Ni³⁺. We observed strong sulfate vibrational modes (34) at ~ 930 cm⁻¹ after the activation step (Fig. 4C), corroborated by TOF-SIMS mapping. Raman spectroscopy also revealed LDH [i.e., α phase-Ni(OH)₂] signatures with TOF-SIMS revealing both sulfate and carbonate ions. These results suggested the formation of a layer of LDH highly enriched with sulfate intercalants formed over NiS_x with abundant sulfate anions outweighing carbonate anions compared with the relative abundance of anions in the NiFe catalyst layer after the same anodic activation. For the activated Ni³⁺ anode, we concluded that the sulfate and carbonate cointercalated NiFe hydroxide catalyst layer together with the underlying sulfate-rich anodized NiS_x layer were responsible for the high OER activity and corrosion resistance to chloride anions in seawater. The NiFe hydroxide layer exhibited higher OER activity than the NiS_x (*SI Appendix, Fig. S12*) and synergized corrosion resistance with the underlying sulfate-rich Ni-Fe-NiS_x interface. Without the electrodeposited NiFe layer, NiS_x/Ni was much less stable for electrolysis in the same salty electrolytes tested (*SI Appendix, Fig. S7A*). This was based on the fact that multivalent anions on hydrous metal oxides surfaces are well known to enhance cation selectivity and afford repulsion and blocking of chloride anions (13, 35, 36). The polyatomic anion (sulfate and carbonate)-passivated Ni³⁺ layers played a critical role in corrosion inhibition by repelling chloride anions and not allowing them to reach and corrode the underlying structure. In addition to electrode

design, we also purposely added sulfate and other polyatomic anions in alkaline seawater electrolytes for electrolysis and also observed stabilization effects for Ni³⁺ and other OER anodes. Hence, careful design of anodes and electrolytes can fully solve the chloride corrosion problem and allow direct splitting of seawater into renewable fuels without desalination.

In summary, we have developed an NiFe/NiS_x/Ni anode for active and stable seawater electrolysis. The uniform electrodeposited NiFe was a highly selective OER catalyst for alkaline seawater splitting, while the NiS_x layer underneath afforded a conductive interlayer and a sulfur source to generate a cation-selective polyatomic anion-rich anode stable against chloride etching/corrosion. The seawater electrolyzer could achieve a current density of 400 mA/cm² under 2.1 V in real seawater or salt-accumulated seawater at room temperature, while only 1.72 V was needed in industrial electrolysis conditions at 80 °C. Critically, the electrolyzer also showed unmatched durability. No obvious activity loss was observed after up to 1,000 h of a stability test. Such a device provides an opportunity to use the vast seawater on Earth as an energy carrier.

Materials and Methods

The materials and methods used in this study are described in detail in *SI Appendix, Materials and Methods*. Information includes synthesis procedures of NiS_x/Ni foam, NiFe/Ni, Ni³⁺, Ni-NiO-Cr₂O₃ cathode, perovskite solar cell fabrication procedure, electrochemical tests details, gas chromatography measurement details, and materials characterization details.

ACKNOWLEDGMENTS. We thank Michael R. Angell for helping to collect spectra data and Andrew Kiss, Doug Van Campen, and Dave Day for support at beamlines 2-2 and 6-2c of the Stanford Synchrotron Radiation Lightsources. This work was partially supported by US Department of Energy (DOE) Grant DE-SC0016165 and National Science Foundation of China, National Key Research and Development Project 2016YFF0204402 (Y.K. and X.S.). Part of this work was performed at the Stanford Nano Shared Facilities, supported by National Science Foundation Grant ECCS-1542152. Use of the Stanford Synchrotron Radiation Lightsources, SLAC National Accelerator Laboratory, is supported by the US DOE, Office of Science, Office of Basic Energy Sciences under Contract DE-AC02-76SF00515.

- Dresselhaus MS, Thomas IL (2001) Alternative energy technologies. *Nature* 414:332–337.
- Dunn B, Kamath H, Tarascon JM (2011) Electrical energy storage for the grid: A battery of choices. *Science* 334:928–935.
- Dunn S (2002) Hydrogen futures: Toward a sustainable energy system. *Int J Hydrogen Energy* 27:235–264.
- Turner JA (2004) Sustainable hydrogen production. *Science* 305:972–974.
- Lewis NS, Nocera DG (2006) Powering the planet: Chemical challenges in solar energy utilization. *Proc Natl Acad Sci USA* 103:15729–15735.
- Walter MG, et al. (2010) Solar water splitting cells. *Chem Rev* 110:6446–6473.
- McCroary CCL, Jung S, Peters JC, Jaramillo TF (2013) Benchmarking heterogeneous electrocatalysts for the oxygen evolution reaction. *J Am Chem Soc* 135:16977–16987.
- Gong M, Wang D-Y, Chen C-C, Hwang B-J, Dai H (2015) A mini review on nickel-based electrocatalysts for alkaline hydrogen evolution reaction. *Nano Res* 9:28–46.
- Zhang J, Chen G, Müllen K, Feng X (2018) Carbon-rich nanomaterials: Fascinating hydrogen and oxygen electrocatalysts. *Adv Mater* 30:e1800528.
- Yang X, et al. (2015) Enabling practical electrocatalyst-assisted photoelectron-chemical water splitting with earth abundant materials. *Nano Res* 8:56–81.
- Dionigi F, Reier T, Pawolek Z, Glich M, Strasser P (2016) Design criteria, operating conditions, and nickel-iron hydroxide catalyst materials for selective seawater electrolysis. *ChemSusChem* 9:962–972.
- van de Krol R, Grätzel M (2012) *Photoelectrochemical Hydrogen Production* (Springer, New York).
- Sharma SK (2011) *Green Corrosion Chemistry and Engineering: Opportunities and Challenges* (Wiley, New York).
- El-Moneim AA, Kumagai N, Hashimoto K (2009) Mn-Mo-W oxide anodes for oxygen evolution in seawater electrolysis for hydrogen production. *Mater Trans* 50:1969–1977.
- Jiang N, Meng H-m (2012) The durability of different elements doped manganese dioxide-coated anodes for oxygen evolution in seawater electrolysis. *Surf Coat Tech* 206:4362–4367.
- Fujimura K, et al. (1999) Anodically deposited manganese-molybdenum oxide anodes with high selectivity for evolving oxygen in electrolysis of seawater. *J Appl Electrochem* 29:769–775.
- Gong M, et al. (2013) An advanced Ni-Fe layered double hydroxide electrocatalyst for water oxidation. *J Am Chem Soc* 135:8452–8455.
- Surendranath Y, Dinca M, Nocera DG (2009) Electrolyte-dependent electrosynthesis and activity of cobalt-based water oxidation catalysts. *J Am Chem Soc* 131:2615–2620.
- Esswein AJ, Surendranath Y, Reece SY, Nocera DG (2011) Highly active cobalt phosphate and borate based oxygen evolving catalysts operating in neutral and natural waters. *Energy Environ Sci* 4:499–504.
- Corrigan DA (1989) Effect of coprecipitated metal ions on the electrochemistry of nickel hydroxide thin films cyclic voltammetry in 1M KOH. *J Electrochem Soc* 136:723–728.
- Corrigan DA (1987) The catalysis of the oxygen evolution reaction by iron impurities in thin film nickel oxide electrodes. *J Electrochem Soc* 134:377–384.
- Gong M, Dai H (2014) A mini review of NiFe-based materials as highly active oxygen evolution reaction electrocatalysts. *Nano Res* 8:23–39.
- Trotochaud L, Young SL, Ranney JK, Boettcher SW (2014) Nickel-iron oxyhydroxide oxygen-evolution electrocatalysts: The role of intentional and incidental iron incorporation. *J Am Chem Soc* 136:6744–6753.
- Xie Q, et al. (2018) Layered double hydroxides with atomic-scale defects for superior electrocatalysis. *Nano Res* 11:4524–4534.
- Lu X, Zhao C (2015) Electrodeposition of hierarchically structured three-dimensional nickel-iron electrodes for efficient oxygen evolution at high current densities. *Nat Commun* 6:6616.
- Gong M, et al. (2015) Blending Cr₂O₃ into a NiO-Ni electrocatalyst for sustained water splitting. *Angew Chem Int Ed Engl* 54:11989–11993.
- Bodner M, Hofer A, Hacker V (2015) H₂ generation from alkaline electrolyzer. *Wiley Interdiscip Rev Energy Environ* 4:365–381.
- Bush KA, et al. (2018) Compositional engineering for efficient wide band gap perovskites with improved stability to photoinduced phase segregation. *ACS Energy Lett* 3:428–435.
- Luo J, et al. (2014) Water photolysis at 12.3% efficiency via perovskite photovoltaics and Earth-abundant catalysts. *Science* 345:1593–1596.
- Louie MW, Bell AT (2013) An investigation of thin-film Ni-Fe oxide catalysts for the electrochemical evolution of oxygen. *J Am Chem Soc* 135:12329–12337.
- Vorsina IA, Mikhailov YI (1996) Kinetics of thermal decomposition of ammonium persulfate. *Russ Chem Bull* 45:539–542.
- Weng LT, Bertrand P, Stone-Masui JH, Stone WEE (1994) ToF SIMS study of the desorption of emulsifiers from polystyrene latexes. *Surf Interface Anal* 21:387–394.
- Zhou D, et al. (2018) Effects of redox-active interlayer anions on the oxygen evolution reactivity of NiFe-layered double hydroxide nanosheets. *Nano Res* 11:1358–1368.
- Tomikawa K, Kanno H (1998) Raman study of sulfuric acid at low temperatures. *J Phys Chem A* 102:6082–6088.
- Sakashita M, Sato N (1979) Ion selectivity of precipitate films affecting passivation and corrosion of metals. *Corrosion* 35:351–355.
- Sakashita M, Sato N (1977) The effect of molybdate anion on the ion-selectivity of hydrous ferric oxide films in chloride solutions. *Corros Sci* 17:473–486.